WEEKDAY EDUCATIONAL COURSE

Everything You Wanted to Know about Magnetic Susceptibility & Why It Is Important

Dmitriy A Yablonskiy, Ph.D. YablonskiyD@wustl.edu

How Magnetic Susceptibility Affects MR Signal Phase in Biological Tissues (Brain)

What is the subject of discussion?

Gradient Recalled Echo (GRE) based MR imaging techniques have wide applications in MRI. Due to the absence of refocusing RF pulses GRE sequences are fast and since low flip angles are usually applied, GRE sequences have low specific absorption rate, hence are particularly well suited for high field MRI. While MR signal generated from GRE techniques is complex, most traditional applications rely only on magnitude information whereas the phase information from the data is usually discarded. However, certain newer applications also rely on phase data. Among these, Susceptibility Weighted Imaging (SWI) (1,2) uses a specific algorithm based on GRE T2* weighted magnitude and phase data to create images sensitive to variations in tissue magnetic susceptibility resulting from sources such as venous blood, calcification, hemorrhage, iron stores, etc. Other techniques, some of which rely exclusively on the phase data of the GRE signal have also been intensely explored for uniquely characterizing anatomical structures that are especially evident at high field MRI (3-6), and even for creating maps of tissue magnetic susceptibility – the so called Quantitative Susceptibility Mapping (QSM) (7-12). Another technique – Gradient Echo Plural Contrast Imaging (GEPCI) (13-15) combines information from phase and magnitude images obtained with multi-gradient-echo sequence to generate a variety of images. The information obtained from these techniques reveals image features complimentary to that obtained from traditional magnitude-based imaging and could improve our understanding of both normal tissue anatomy as well as changes in tissue in various pathological conditions.

To appreciate the information obtained from phase images, we need to understand biophysical mechanisms that affect GRE signal phase. For GRE experiment with gradient echo time *TE* this phase is $\varphi(TE) = \varphi_0 + 2\pi f \cdot TE$, where f is a local Larmor resonance frequency and φ_0 is initial signal phase. The magnetic resonance frequency f of a spin in a tissue can be described by several additive components:

$$f = f_0 - \sigma \cdot f_0 + \delta f_e + \delta f_\chi . \quad (1)$$

(i) a component $f_0 = \gamma \cdot B_0$ is the base Larmor resonance frequency, where γ is the gyromagnetic ratio (MHz/T) and B_0 is the main static field, (ii) a component $-\sigma f_0$ is due to the local, electronic shielding provided by the "host" water molecule (shielding factor σ) (iii) a component δf_e is due to chemical exchange between free (bulk) water and bound water, typically that associated with hydrophilic groups on the surface (and perhaps interior) of macromolecules (6,16,17), and (iv) a component δf_χ is due to the magnetic susceptibility of the tissue. This last term is the subject of our discussion.

Proc. Intl. Soc. Mag. Reson. Med. 22 (2014)

What is the problem?

From the "magnetic perspective", the main biological tissue components (proteins, lipids, iron, etc.) act as magnetic susceptibility inclusions in the tissue water. In an external magnetic field $B_{0,}$ magnetic susceptibility inclusions become magnetized and create their own magnetic fields. Since these induced magnetic fields decay relatively slow with distance, they affect (shift) not only Larmor resonance frequencies of neighboring water molecules but also distant neighbors. Consequently, the Larmor resonance frequency of a given water molecule is also affected by magnetic fields created by numerous susceptibility inclusions located near this molecule and far away. Calculating this frequency is usually a very difficult problem.

How this problem can be addressed?

Even though exact solution to this problem is not possible, a substantial simplification can be achieved using approach similar to proposed a century ago by Lorentz (18) (see also discussion in (19)).

It is useful to start our discussion using citation from Lorentz 1909 publication:

"If we want to know the field produced at a point *A* by a part of the body whose shortest distance from *A* is very great compared with the mutual distance of adjacent particles, we may replace the real state of things by one in which the polarized matter is homogeneously distributed."

"Around the particle *A* for which we wish to determine the action exerted on the electron it contains, we lay a closed surface σ, whose dimensions are infinitely small in a physical sense, and we conceive, for a moment, all other particles lying within this surface to be removed. The state of things is then exactly analogous to the case of magnet in which a cavity has been formed. There will be a distribution of electricity on the surface, due to the polarization of the outside portion of the body, and the force $\mathbf{E}'$, exerted by this distribution on a unit charge *A* must be added to the force **E.**

Now, if the particles we have just removed are restored to their places, their electric moments will produce a third force $\mathbf{E}''$ in the particle *A*, and total electric force to which the movable electron of *A* is exposed, will be

$$\mathbf{E}+\mathbf{E}'+\mathbf{E}''.$$

It is clear that the result cannot depend on the form of the cavity σ, which has only been imagined for the purpose of performing the calculations. These take the simplest form if σ is a sphere. Then calculations of the force $\mathbf{E}'$ lead to the result

$$\mathbf{E}'=\frac{1}{3}\mathbf{P}$$

The problem of determining the force $\mathbf{E}''$ is more difficult. I shall not dwell upon it here, and shall only say that, for a system of particles having a regular cubical arrangement, one finds

$$\mathbf{E}''=0,$$

a result that can be applied with a certain degree of approximation to isotropic bodies in general, such as glass, fluids and gases. It is not quite correct however for these, and ought to be replaced in general by

$$\mathbf{E}''=s\mathbf{P},$$

where, for each body, *s* is a constant which will be difficult exactly to determine."

Lorentz, The theory of electrons, 1909 (18).

There are several points that we would like to underline from Lorentz' consideration (note that the electric field **E** is an analog of magnetic field **H**):

1. There are no real physical empty spheres (or any other cavities) in the body under consideration – the surface σ surrounding point of interest A in Lorentz consideration is an imaginary surface.
2. A commonly used assumption that the size of Lorentzian surface can be selected arbitrary small is not valid! The size of this surface should be much bigger "compared with the mutual distance of adjacent particles" (magnetic susceptibility inclusions in our case). In this case the field created by particles outside the surface can be calculated as a field produced by homogeneous media.
3. The shape of the surface can be arbitrary as long as the total Lorentz field

$$\mathbf{H}^L = \mathbf{H}' + \mathbf{H}'' \quad [2]$$

is calculated. The result for the total $\mathbf{H}^L$ in Eq. [2] should not depend on this shape.
4. Utmost important - the field $\mathbf{H}''$ created by particles located inside the surface is generally not zero"!

In the current MRI literature (e.g. (20)) it is assumed that the frequency shift δf due to the presence of magnetic susceptibility inclusions can be calculated as

$$\frac{\delta f}{f_0} = \frac{1}{3}\chi \quad [3]$$

where f_0 is the base frequency of the MRI scanner and χ is a total magnetic susceptibility of the tissue. According to Lorentz, this can be true if: i) we would use the spherical surface σ (Lorentzian sphere, as it is called in the current literature) and ii) the contribution $\mathbf{H}''$ from all the susceptibility inclusions inside this sphere would be zero.

It was demonstrated in (21) that in biological tissues the magnetic susceptibility induced frequency shift depends not only on tissue total magnetic susceptibility χ, but also on tissue "magnetic architecture" – distribution of magnetic susceptibility inclusions at the cellular and sub-cellular levels. It was shown in (21) that the relationship in Eq. [3] is incorrect when magnetic susceptibility inclusions form longitudinal structures with their lengths much bigger than their transverse dimensions and average distance between them. Examples of longitudinal structures in the brain tissue are neurofilaments inside the axons and myelin layers covering the axons.

In the original paper (21) and follow-up publications (22-24) Lorentzian principles were used to establish the relationship between the gradient echo MRI signal phase/frequency and underlying biological tissue microstructure at the cellular and sub-cellular levels. Figure 1 provides illustration of these ideas and methods.

An illustration what happenings when using Lorentzian spherical surface in the case of longitudinal structures is shown in Fig. 1, upper row. We can see from this figure that the magnetic field created by the magnetostatic charges on the surface σ of the Lorentzian sphere is indeed

$$\mathbf{H}' = \frac{1}{3}\mathbf{M} = \frac{1}{3}\chi \cdot \mathbf{B}_0 \quad [4]$$

where $\mathbf{M}$ is a volume magnetization, and χ is a contribution to the volume magnetic susceptibility of the system from the longitudinal inclusions. However, the field $\mathbf{H}''$ induced by the magnetic susceptibility inclusions remaining inside the Lorentzian sphere, is exactly opposite to $\mathbf{H}'$ in Eq. [4]:

$$\mathbf{H}'' = -\frac{1}{3}\mathbf{M} = -\frac{1}{3}\chi \cdot \mathbf{B}_0 \quad [5]$$

because their magnetostatic charges are equal in value and opposite in sign to the magnetostatic charges determining the field $\mathbf{H}'$. Thus, as expected, the Lorentz field

$$\mathbf{H}^L_{long} = \mathbf{H}' + \mathbf{H}'' = 0 \quad [6]$$

Hence, Eq. [3] is not valid in this case.

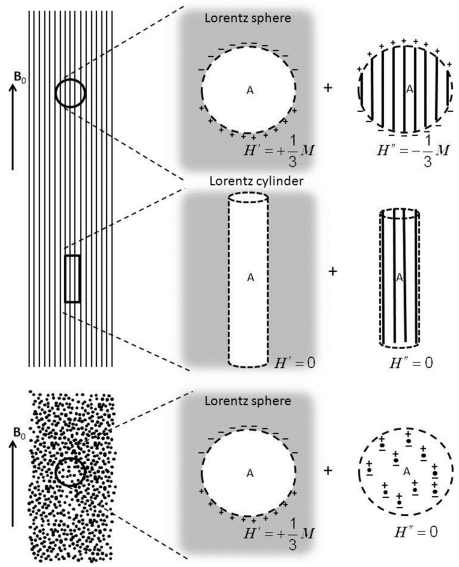

Figure 1. Lorentzian magnetic field for two types of magnetic susceptibility inclusions: longitudinal, shown as solid rods, and isotropic, shown as solid spheres. In the presence of $\mathbf{B}_0$, the average volume magnetization of the tissue is $\mathbf{M} = \chi \mathbf{B}_0$. The Lorentzian magnetic field $\mathbf{H}^L$ is a sum of the contributions induced by the part of the inclusions outside the surface, $\mathbf{H}'$ (middle column), and inside the surface, $\mathbf{H}''$ (right column): $\mathbf{H}^L = \mathbf{H}' + \mathbf{H}''$. Following Lorentz, the magnetization outside the surface is considered as homogeneous.
Upper row: *Longitudinally arrange inclusions and spherical surface*. The radius of the sphere must be chosen much bigger than the average distance between the rods but much smaller than their length. The fields $\mathbf{H}'$ and $\mathbf{H}''$ are determined by the surface magnetostatic charges $\rho = -\mathrm{div}\,\mathbf{M} = -\partial M / \partial z$ (z-axis is parallel to the external field $\mathbf{B}_0$), which exist on the cross sections of the rods and spherical surface. Their signs are denoted by "+" and "–". The field $\mathbf{H}'$ is created by the surface charge that is negative on the upper hemisphere and positive on the lower hemisphere. As in the electrostatic problem considered by Lorentz, $\mathbf{H}' = \mathbf{M}/3$. Importantly, the field $\mathbf{H}''$ is not zero: $\mathbf{H}'' = -\mathbf{M}/3$ since it is determined by the same magnetostatic charges as $\mathbf{H}'$ but of the opposite sign. Thus, both the fields $\mathbf{H}'$ and $\mathbf{H}''$ are non-zero but compensate each other, and $\mathbf{H}^L = 0$. **Middle row**: *Longitudinally arrange inclusions and cylindrical surface*. In this case, no magnetostatic charges are induced and both the fields $\mathbf{H}'$ and $\mathbf{H}''$ are equal to zero. Hence, $\mathbf{H}^L = 0$ automatically, emphasizing the convenience of selecting Lorentzian cylinder for this case (21). **Lower row**: *Spherical uniformly distributed inclusions and spherical surface*. The field $\mathbf{H}' = \mathbf{M}/3$ as the magnetization outside the cavity is considered as homogeneously distributed. In contrast to the longitudinally arrange inclusions, the field $\mathbf{H}'' = 0$ due to the uniform distribution of the inclusions and the fact that an average magnetic field around magnetized spherical particle is zero (this result is also confirmed by computer simulations in (22)). Thus, the Lorentzian field $\mathbf{H}^L$ is equal to $\mathbf{H}^L = \mathbf{M}/3$.

As was proposed in (21), for longitudinal structures, a natural choice of Lorentzian surface is a cylinder encompassing them, as shown in Fig. 1, middle row. In this case, no structures cross Lorentzian surface, no magnetostatic charges exist and both the fields ($\mathbf{H}'$ and $\mathbf{H}''$) are automatically zero:

$$\mathbf{H}' = 0, \quad \mathbf{H}'' = 0, \quad \mathbf{H}^L_{long} = 0 \qquad [7]$$

The situation is different in case of isotropically distributed magnetic susceptibility inclusions of the spherical shape. This is illustrated in Fig. 1, lower row. A natural choice of Lorentzian surface is now sphere; the field $\mathbf{H}'$ is given by Eq. [4], the field $\mathbf{H}''$ is now zero, hence:

$$\mathbf{H}^L_{iso} = \mathbf{H}' = \frac{1}{3}\mathbf{M} = \frac{1}{3}\chi \cdot \mathbf{B}_0 \qquad [8]$$

In the general case when we have both sphere-like and longitudinal magnetic susceptibility inclusions with external magnetic field $\mathbf{B}_0$ forming an angle α with the axis of longitudinal structures, our theory, that we call Generalized Lorentzian Approach (GLA) (21), suggests that the frequency shift due to the Lorentzian field is:

$$\left.\frac{\delta f}{f_0}\right|_{GLA} = \frac{1}{3}\chi_i + \frac{1}{2}\chi_{long} \cdot \sin^2\alpha \qquad [9]$$

where χ_i is a contribution to the tissue volume magnetic susceptibility from uniformly distributed spherical-like (isotropic) objects and χ_{long} is a contribution from the longitudinal structures. The coefficients 1/3 and 1/2 in Eq. [9] result from demagnetizing factors of sphere and cylinder, correspondingly (25). Hence, for cylindrical structures, the Lorentzian field contribution to the frequency shift is the same *as if water molecules would be residing in a hollow cylinder* with magnetic susceptibility χ_{long}, Eq. [9], second term, and for randomly distributed spheres – the result is the same *as if water*

molecules would be residing inside a hollow sphere with magnetic susceptibility χ_i, Eq. [9], first term. The "*imaginary hollow space*" appears because in both cases an average magnetic field around either 3D (point) dipole or 2D (line) dipole is zero (21).

While GLA has already predicted anisotropic behavior of GRE signal phase (21), it was suggested later (26,27) that the magnetic susceptibility of myelin can be anisotropic. This effect can also be incorporated in the GLA. By making a reasonable assumption that the anisotropic magnetic susceptibility can be attributed to longitudinal structures and can be characterized by two components – axial, $\chi_{\parallel}$, and radial, $\chi_{\perp}$, we arrive to the following modification of Eq. [9]:

$$\mathbf{H}_{GLA} = \frac{1}{3}\chi_i \cdot \mathbf{B}_0 + \frac{1}{2}\hat{\Lambda} \cdot \mathbf{B}_0 \qquad [10]$$

where tensor $\hat{\Lambda}$ has only two non-zero components, $\Lambda_{xx} = \Lambda_{yy} = \chi_{\perp}$ in the system of coordinates where *Z*-axis is parallel to the direction of longitudinal structures. At the same time, the tissue magnetization is defined as

$$\mathbf{M} = \chi_i \cdot \mathbf{B}_0 + \hat{\chi}_{long} \cdot \mathbf{B}_0 \qquad [11]$$

where the magnetic susceptibility tensor $\hat{\chi}_{long}$ has three components ($\chi_{long,xx} = \chi_{long,yy} = \chi_{\perp}$, $\chi_{long,zz} = \chi_{\parallel}$) in the same system of coordinates. The set of equations [10] and [11] is different from proposed in (26). In our approach, only transverse components of magnetic susceptibility tensor contribute to Lorentzian field in Eq. [10] (longitudinal components are "invisible"), while all the components contribute to the tissue magnetization in Eq. [11].

It can be shown that for a system comprising multiple types of susceptibility inclusions with volume fractions λ_n and described by the demagnetizing tensors $\hat{\mathbf{N}}_n$ and magnetic susceptibility tensors $\hat{\chi}_n$, respectively, the general expression for the Lorentzian field is a sum over all components:

$$\mathbf{H}_{GLA} = \sum_n \lambda_n \cdot \hat{\mathbf{\Lambda}}_n \cdot \mathbf{B}_0, \quad \hat{\mathbf{\Lambda}}_n = \hat{\mathbf{N}}_n \cdot \hat{\chi}_n \qquad [12]$$

All the above consideration is based on the assumption that tissue can be considered in the framework of a single component model with impermeable magnetic susceptibility inclusions. More sophisticated analytical (24,28) and numerical (29) multi-component models of brain tissue have recently been developed. In a linear approximation, their results can be reduced to the equations described above with all the coefficients treated as apparent.

Conclusion: The consideration above explains the ideas and the results of GLA that are based on the principles formulated by Lorentz (18). They are in agreement with an exact theoretical consideration (13), they are backed up by computer simulations in (22) and have been experimentally validated in a carefully designed experiment with the optic nerve (23). Recall, that there are no actual spheres or ellipsoids in the biological tissue. The surfaces proposed by Lorentz are imaginary and only needed to calculate fields created by numerous susceptibility inclusions by separating contribution from near environment and the remote sources. Since the total field at any point is a sum of the fields created by all the susceptibility inclusions, it is natural to calculate the part of the field created by sphere-like inclusions using Lorentzian sphere, and the part of the field created by longitudinal structures – using Lorentzian cylinder. The relationship between the gradient echo MR signal phase and underlying tissue magnetic susceptibility can only be described in terms of Lorentzian sphere for randomly distributed sphere-like susceptibility inclusions. In the brain where long cells (axons, etc.) are present, the GLA is the essential tool that connects MR signal phase with the underlying tissue microstructure (magnetic architecture).

References

1. Reichenbach JR, Venkatesan R, Schillinger DJ, Kido DK, Haacke EM. Small vessels in the human brain: MR venography with deoxyhemoglobin as an intrinsic contrast agent. Radiology 1997;204(1):272-277.
2. Haacke EM, Mittal S, Wu Z, Neelavalli J, Cheng YCN. Susceptibility-Weighted Imaging: Technical Aspects and Clinical Applications, Part 1. American Journal of Neuroradiology 2009;30(1):19-30.
3. Rauscher A, Sedlacik J, Barth M, Mentzel HJ, Reichenbach JR. Magnetic susceptibility-weighted MR phase imaging of the human brain. AJNR Am J Neuroradiol 2005;26(4):736-742.
4. Duyn JH, van Gelderen P, Li TQ, de Zwart JA, Koretsky AP, Fukunaga M. High-field MRI of brain cortical substructure based on signal phase. Proceedings of the National Academy of Sciences of the United States of America 2007;104(28):11796-11801.
5. Marques JP, Maddage R, Mlynarik V, Gruetter R. On the origin of the MR image phase contrast: An in vivo MR microscopy study of the rat brain at 14.1 T. Neuroimage 2009;46(2):345-352.
6. Zhong K, Leupold J, von Elverfeldt D, Speck O. The molecular basis for gray and white matter contrast in phase imaging. Neuroimage 2008;40(4):1561-1566.
7. de Rochefort L, Brown R, Prince MR, Wang Y. Quantitative MR susceptibility mapping using piece-wise constant regularized inversion of the magnetic field. Magnetic Resonance in Medicine 2008;60(4):1003-1009.
8. Liu TA, Spincemaille P, de Rochefort L, Wong R, Prince M, Wang Y. Unambiguous identification of superparamagnetic iron oxide particles through quantitative susceptibility mapping of the nonlinear response to magnetic fields. Magnetic Resonance Imaging 2010;28(9):1383-1389.
9. Shmueli K, De Zwart JA, Van Gelderen P, Li TQ, Dodd SJ, Duyn JH. Magnetic susceptibility mapping of brain tissue in vivo using MRI phase data. Magnetic Resonance in Medicine 2009;62(6):1510-1522.
10. Schweser F, Deistung A, Lehr BW, Reichenbach JR. Differentiation between diamagnetic and paramagnetic cerebral lesions based on magnetic susceptibility mapping. Medical Physics 2010;37(10):5165-5178.
11. de Rochefort L, Liu T, Kressler B, Liu J, Spincemaille P, Lebon V, Wu JL, Wang Y. Quantitative Susceptibility Map Reconstruction from MR Phase Data Using Bayesian Regularization: Validation and Application to Brain Imaging. Magnetic Resonance in Medicine 2010;63(1):194-206.
12. Li W, Wu B, Liu CL. Quantitative susceptibility mapping of human brain reflects spatial variation in tissue composition. Neuroimage 2011;55(4):1645-1656.
13. Yablonskiy DA, Haacke EM. Theory of NMR signal behavior in magnetically inhomogeneous tissues: the static dephasing regime. Magn Reson Med 1994;32(6):749-763.
14. Sati P, Cross AH, Luo J, Hildebolt CF, Yablonskiy DA. In vivo quantitative evaluation of brain tissue damage in multiple sclerosis using gradient echo plural contrast imaging technique. Neuroimage 2010;51(3):1089-1097.
15. Luo J, Jagadeesan BD, Cross AH, Yablonskiy DA. Gradient Echo Plural Contrast Imaging - Signal model and derived contrasts: T2*, T1, Phase, SWI, T1f, FST2*and T2*-SWI. Neuroimage 2012;60(2):1073-1082.
16. Luo J, He X, d'Avignon DA, Ackerman JJH, Yablonskiy DA. Protein-induced water H-1 MR frequency shifts: Contributions from magnetic susceptibility and exchange effects. Journal of Magnetic Resonance 2010;202(1):102-108.
17. Shmueli K, Dodd SJ, Li TQ, Duyn JH. The Contribution of Chemical Exchange to MRI Frequency Shifts in Brain Tissue. Magnetic Resonance in Medicine 2011;65(1):35-43.
18. Lorentz HA. The Theory of Electrons. . Leipzig, New York: B.G. Teubners; 1909. p 133.
19. Yablonskiy DA, He X, Luo J, Sukstanskii AL. Lorentzian Sphere vs. Generalized Lorentzian Approach: What Woul Lorentz Say About This. Mag Res Med 2014.
20. Chu SC, Xu Y, Balschi JA, Springer CS, Jr. Bulk magnetic susceptibility shifts in NMR studies of compartmentalized samples: use of paramagnetic reagents. Magn Reson Med 1990;13(2):239-262.
21. He X, Yablonskiy DA. Biophysical mechanisms of phase contrast in gradient echo MRI. Proceedings of the National Academy of Sciences of the United States of America 2009;106(32):13558-13563.
22. Yablonskiy DA, Luo J, Sukstanskii AL, Iyer A, Cross AH. Biophysical mechanisms of MRI signal frequency contrast in multiple sclerosis. Proc Natl Acad Sci U S A 2012;109(35):14212-14217.
23. Luo J, He X, Yablonskiy DA. Magnetic susceptibility induced white matter MR signal frequency shifts-experimental comparison between Lorentzian sphere and generalized Lorentzian approaches. Magn Reson Med 2013;DOI:10.1002/mrm.24762.
24. Sukstanskii AL, Yablonskiy DA. On the role of neuronal magnetic susceptibility and structure symmetry on gradient echo MR signal formation. Magnetic Resonance in Medicine 2013:DOI 10.1002/mrm.24629.
25. Osborn J. Demagnetizing Factors of the General Ellipsoid. Physical Review 1945;67:351-357.
26. Liu CL. Susceptibility Tensor Imaging. Magnetic Resonance in Medicine 2010;63(6):1471-1477.
27. Lee J, Shmueli K, Fukunaga M, van Gelderen P, Merkle H, Silva AC, Duyn JH. Sensitivity of MRI resonance frequency to the orientation of brain tissue microstructure. Proceedings of the National Academy of Sciences of the United States of America 2010;107(11):5130-5135.
28. Wharton S, Bowtell R. Fiber orientation-dependent white matter contrast in gradient echo MRI. Proc Natl Acad Sci U S A 2012;109(45):18559-18564.
29. Sati P, van Gelderen P, Silva AC, Reich DS, Merkle H, de Zwart JA, Duyn JH. Micro-compartment specific T2* relaxation in the brain. Neuroimage 2013;77(0):268-278.